


# Multi-Frequency, MW-Power Triode Gyrotron Having a Uniform Directional Beam

Ryosuke Ikeda<sup>1</sup>  · Yasuhisa Oda<sup>1</sup> ·  
Takayuki Kobayashi<sup>1</sup> · Ken Kajiwara<sup>1</sup> ·  
Masayuki Terakado<sup>1</sup> · Koji Takahashi<sup>1</sup> ·  
Shinichi Moriyama<sup>1</sup> · Keishi Sakamoto<sup>1</sup>

Received: 29 August 2016 / Accepted: 7 December 2016 /  
Published online: 14 December 2016  
© Springer Science+Business Media New York 2016

## 1 Introduction

A gyrotron is an efficient power source in the millimeter wave region and is used in fusion, material, and life sciences. Especially in fusion science high-power gyrotrons, around 1 MW have become indispensable for electron heating and current drive to control high-temperature plasmas. The International Thermonuclear Experimental Reactor (ITER) project uses 24, 170 GHz/1 MW gyrotrons for electron heating and current drive and for suppressing neoclassical tearing modes [1–4]. In plasma confinement devices, multi-frequency oscillation of high-power gyrotrons is ideal for controlling plasma at magnetic fields of varying strength without the need for additional components. Multi-frequency oscillation is also useful to study heat transport physics in various magnetic field conditions using power modulation and wave physics such as electron heating and current drive using harmonic electron cyclotron waves or electron Bernstein waves in over-dense plasmas. We designed and developed a 137 GHz/170 GHz dual-frequency gyrotron having a single diamond window and a triode magnetron injection gun (MIG) [5]. In gyrotrons having a conventional single disc window, the transparent frequencies are determined by the thickness of the window. Now, dual-frequency gyrotrons having a single window have been developed [6, 7]. Gyrotrons having a Brewster angle window that has a wide frequency range are also being developed [8, 9]. In either case, the RF beam radiated from the gyrotron output window has varying radiation angles. Therefore, it will be necessary to align the mirror angle in a matching optics unit (MOU) to effectively transmit the RF beam power for each oscillation frequency into a transmission waveguide. To minimize

---

✉ Ryosuke Ikeda  
ikeda.ryosuke@qst.go.jp

<sup>1</sup> National Institutes for Quantum and Radiological Science and Technology (QST), Naka, Ibaraki 311-0193, Japan

this issue, we developed a multi-frequency, MW-power gyrotron having a uniform directional beam by selecting a unique oscillation mode group.

## 2 Design of Multi-Frequency Gyrotron

The design of the multi-frequency gyrotron must satisfy the requirements for the output window, cavity resonator, and mode converter. With a conventional single window, the window thickness should be the half-integer multiple of the wavelength in the window,  $\lambda_w$ , to transmit the RF beam. There are many  $TE_{m,n}$  modes excited for various electron beam radii and magnetic field strengths at the cavity resonator; however, in practice, the adjustable range of the beam radius is limited. It is preferred that the beam radii for sub-modes be close to the value of the main mode the gyrotron was designed for to avoid the electron beam striking the entrance of the cavity resonator or the mode converter. The transverse radiation angle of the RF beam in the mode converter is also important. The transverse radiation angle can be described as  $\theta_{\text{rad}} = N_r \cos^{-1}(m/\chi_{m,n})$ , where  $N_r$  is the number of reflections in the mode converter, and  $\chi_{m,n}$  is the  $n$ th root of the  $m$ th order derivative Bessel function. It is desirable for the values of  $m_{\text{sub}}/\chi_{m,n_{\text{sub}}}$  for sub-mode to be close to the value of  $m_{\text{main}}/\chi_{m,n_{\text{main}}}$  for the main mode. The gap of the radiation angle is described as:

$$\Delta\theta_{\text{rad}} = N_r \left( \cos^{-1} \left( \frac{m_{\text{main}}}{\chi_{m,n_{\text{main}}}} \right) - \cos^{-1} \left( \frac{m_{\text{sub}}}{\chi_{m,n_{\text{sub}}}} \right) \right).$$

As this gap angle is smaller, the RF beam radiated for each frequency propagates to similar direction. The gap angle in some special mode groups is close to zero, and a  $TE_{19,7}$ - $TE_{25,9}$ - $TE_{31,11}$ - $TE_{37,13}$  mode group satisfied this condition. Therefore, to deliver a multi-frequency gyrotron having a uniform directional beam, the  $TE_{31,11}$  mode for 170 GHz oscillation was selected. In addition, this 170 GHz oscillation of  $TE_{31,11}$  mode has a margin for thermal loading in the cavity resonator when operating at 1 MW output power. We have already developed a  $TE_{31,8}$  mode gyrotron equipped with a triode MIG that has demonstrated high performance, e.g., 1 MW output power and 55% total electric efficiency [10]. Therefore, it was not necessary to design a new MIG because the optimal beam radius at the cavity resonator is the same. To excite the  $TE_{31,11}$  mode of 170 GHz, the radius of the cavity resonator and the optimal beam radius at the cavity resonator are 20.87 and 9.13 mm, respectively. The thickness of the output window, made of chemical vapor deposition (CVD) diamond, is 1.853 mm to perfectly transmit the 170 GHz RF beam, which corresponds to  $5\lambda_w/2$ . The transparent frequency,  $f_w$ , and the wavelength in the window are described as  $f_w = Nc\lambda_w/2\lambda_0$  and  $\lambda_w = \lambda_0/\sqrt{\epsilon}$ . Here,  $c$  is the light speed,  $N$  is an integer,  $\lambda_0$  is vacuum wavelength, and  $\epsilon$  is a relative permittivity of diamond. Oscillation frequencies for  $TE_{19,7}$ ,  $TE_{25,9}$ , and  $TE_{37,13}$  modes are 104, 137, and 203 GHz, respectively, and are close to the transparent frequencies 102 GHz ( $3\lambda_w/2$ ), 136 GHz ( $4\lambda_w/2$ ), and 204 GHz ( $6\lambda_w/2$ ), respectively. The electron beam radii are 9.25 mm for  $TE_{19,7}$  mode, 9.19 mm for  $TE_{25,9}$  mode, and 9.10 mm for  $TE_{37,13}$  mode. The values of the radiation angle are  $65.30^\circ$  for  $TE_{19,7}$  mode,  $65.32^\circ$  for  $TE_{25,9}$  mode,  $65.35^\circ$  for  $TE_{31,11}$  mode, and  $65.37^\circ$  for  $TE_{37,13}$  mode. These values are summarized in Table 1. Since the RF beam radiated from the output window is uniform for each frequency, the RF beam power is coupled to the transmission waveguide without having to align the two mirrors in the MOU for each frequency. In addition, triode gyrotrons are suitable for multi-frequency

**Table 1** Beam radius, oscillation frequency, window transparent frequency, and radiation angle in mode converter for each cavity oscillation mode (cavity radius, 20.87 mm; diamond window thickness, 1.853 mm)

$TE_{m,n}$ mode	Beam radius (mm)	Oscillation frequency (GHz)	Transparent frequency (GHz)	Radiation angle (°)
19,7	9.10	104	102 GHz ( $=3/2\lambda_w$ )	65.3003
25,9	9.13	137	136 GHz ( $=4/2\lambda_w$ )	65.3235
31,11	9.19	170	170 GHz ( $=5/2\lambda_w$ )	65.3492
37,13	9.25	203	204 GHz ( $=6/2\lambda_w$ )	65.3665

oscillation because the beam voltage  $V_{beam}$ , velocity ratio (pitch factor)  $\alpha$ , and beam radius  $R_b$ , can be selected independently. The pitch factor and the beam radius are described as follows [11]:

$$\alpha = \frac{v_{\perp 0}}{v_{\parallel 0}} = \frac{\beta_{\perp 0}}{(1-\gamma_0^{-2}-\beta_{\perp 0}^2)^{1/2}}, \beta_{\perp 0} = \frac{b^{3/2}E_c \cos\phi_c}{cB_c\gamma_0} \text{ and } R_b = \frac{R_e}{b^{1/2}}.$$

Here,  $v_{\perp 0}$  and  $v_{\parallel 0}$  are perpendicular and parallel components of electron velocity;  $\beta_{\perp 0}$  ( $=v_{\perp 0}/c$ ) is normalized perpendicular velocity for light speed;  $\gamma_0$  ( $\sim 1 + V_{beam}/511$ ) is the relativistic mass factor;  $b$  is the magnetic compression ratio between the magnetic field strength around the cavity resonator and the MIG;  $\phi_c$  is a cathode slant angle;  $B_c$  is the magnetic field strength around MIG;  $E_c$  is the electric field around the MIG; and  $R_e$  is the emitter radius in the MIG. In diode gyrotrons,  $E_c$  is a function of the beam voltage and in triode gyrotrons,  $E_c$  is a function of the voltage between anode and cathode electrodes (anode–cathode voltage,  $V_{ac}$ ). The beam radius is adjusted by a gun coil magnet around the MIG. With triode gyrotrons, even if the magnetic compression ratio and beam radius is changed to excite other modes, the pitch factor can be optimized by the anode–cathode voltage. On the other hand, in the cases of gyrotrons equipped with a diode MIG, the beam voltage must be changed to obtain the same pitch factor for each mode because the relativistic mass factor is also a function of the beam voltage. Numerical analysis for oscillations of 104, 137, 170, and 203 GHz are shown in Table 2. In these calculations, the pitch factors for all frequencies are about 1.35 when the beam voltage and the beam current are 72 kV and 40 A, respectively. The oscillation power and oscillation efficiency at the cavity resonator are 1.30 MW/45% for 170 and 203 GHz, 1.26 MW/44% for 137 GHz, and 1.12 MW/39% for 104 GHz. Triode gyrotrons can easily obtain the optimal oscillation conditions for any oscillation mode.

**Table 2** Designed oscillation power and oscillation efficiency at a cavity resonator for four frequencies (beam voltage, 72 kV; beam current, 40 A)

Oscillation frequency	104 GHz	137 GHz	170 GHz	203 GHz
Cavity field	4.08 T	5.32 T	6.63 T	7.98 T
Gun field	0.17 T	0.21 T	0.28 T	0.31 T
Beam radius	9.25 mm	9.19 T	9.13 mm	9.10 mm
Anode–cathode voltage	28 kV	36 kV	42 kV	50 kV
Pitch factor	1.32	1.35	1.35	1.35
Oscillation power	1.12 MW	1.26 MW	1.30 MW	1.30 MW
Oscillation efficiency	39%	44%	45%	45%

### 3 Results of Experiments Using Multi-Frequency Oscillations

The detailed specifications of this  $TE_{31,11}$  mode gyrotron are given in reference [12]. The design of the mode converter and four internal mirrors in the gyrotron is optimized for  $TE_{31,11}$  mode of 170 GHz oscillation using the design software Lot/Surf3D. The designed beam patterns at the front of the output window for  $TE_{19,7}$  mode,  $TE_{25,9}$  mode,  $TE_{31,11}$  mode, and  $TE_{37,13}$  mode are shown in Fig. 1a–d. Here, the window aperture is 80 mm. The main power ( $> -10$  dB) was fitted in the window aperture for each mode. However, lower power components ( $< -20$  dB) are not fitted in low frequency mode and internal stray power is increased. Design transmission efficiencies from the internal mode converter to the output window are 98.5% for main 170 GHz, 97.6% for 203 GHz, 96.9% for 137 GHz, and 95.5% for 104 GHz. Radiation beam profiles were measured using an infrared camera as the temperature rose on a target paper screen in short-pulse durations ( $< 1$  ms). Figure 1e–h shows logarithmic-scaled profiles that are normalized by the peak temperature for each mode. These measured oscillation frequencies were 202.97 GHz for  $TE_{37,13}$  mode, 169.98 GHz for  $TE_{31,11}$  mode, 137.04 GHz for  $TE_{25,9}$  mode, and 104.05 GHz for  $TE_{19,7}$  mode. The radiation direction of the RF beam was aligned for  $TE_{31,11}$  mode by a final mirror in the gyrotron and the beam passed through the center of the diamond window. The observed beam pattern was a clear Gaussian-like beam and the main beam profile was in good agreement with the calculations as shown in Fig. 1g. The beam power up to  $-20$  dB was also fitted in the window aperture. The measured beam profile of  $TE_{37,13}$  mode was almost the same as that of  $TE_{31,11}$  mode, and the beam power was also fitted in the aperture. The main power ( $> -10$  dB) for  $TE_{25,9}$  mode and  $TE_{19,7}$  mode passed through the center of the diamond window and beam profiles similar to the calculation patterns were observed. On the other hand, the lower power of  $-20$  dB was on the edge of the aperture in the  $TE_{25,9}$  mode and was outside of the aperture in the  $TE_{19,7}$  mode. Therefore, some degree of stray power in the gyrotron will be increased.

The quad-frequency oscillations were conducted at high power. The operation conditions, output power, and efficiencies achieved are summarized in Table 3. The output power for  $TE_{31,11}$  mode achieved  $P_{out} = 1.21$  MW for 2 s pulses with the magnetic field at cavity resonator

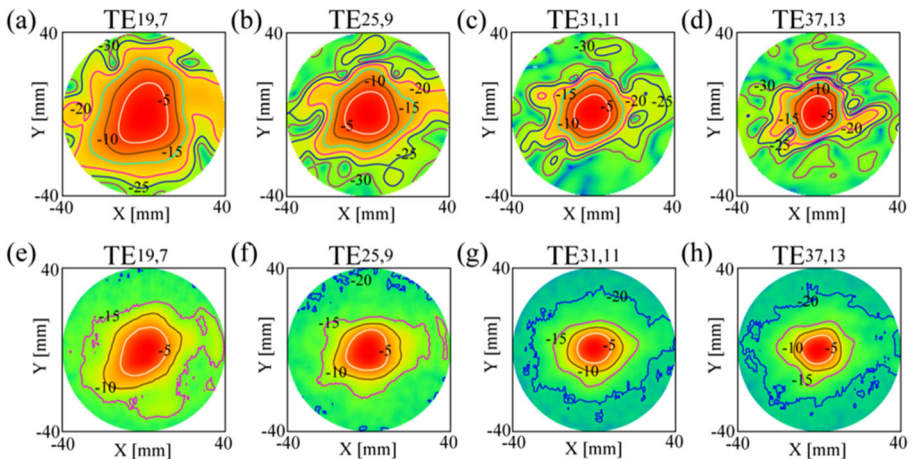


**Fig. 1** Designed beam profiles (logarithmic scale) for  $TE_{19,7}$ ,  $TE_{25,9}$ ,  $TE_{31,11}$ , and  $TE_{37,13}$  modes at output window (a–d) and measured beam profiles (logarithmic scale) for each mode (e–h)

**Table 3** Achieved output power and efficiency for quad-frequency oscillation

TE <sub><i>m,n</i></sub> mode	19,7	25,9	31,11	37,13
Oscillation frequency	103.9 GHz	136.8 GHz	169.9 GHz	202.8 GHz
Output power	1.03 MW	1.00 MW	1.21 MW	0.42 MW
Output efficiency	25.5%	25.4%	27.5%	25.1%
Total electric efficiency	40.0%	41.3%	45.0%	38.5%
Cavity field	4.04 T	5.34 T	6.66 T	7.94 T
Beam voltage	76 kV	76 kV	80 kV	72 kV
CPD voltage	27.5 kV	29.5 kV	31.5 kV	25.0 kV
Anode–cathode voltage	25.0 kV	34.5 kV	44.0 kV	45.0 kV
Beam current	53 A	52 A	55 A	23.5 A
Pulse length	2 s	2 s	2 s	5 s

$B_0 = 6.66$  T, beam voltage  $V_{\text{beam}} = 80$  kV, and beam current  $I_{\text{beam}} = 55$  A. An output efficiency ( $\eta_{\text{out}} = P_{\text{out}}/I_{\text{beam}}V_{\text{beam}}$ ) was 27.5% and a total electric efficiency ( $\eta_{\text{tot}} = P_{\text{out}}/I_{\text{beam}}(V_{\text{beam}} - V_{\text{CPD}})$ ) was 45% using a collector potential depression (CPD) voltage,  $V_{\text{CPD}}$ . At present, 1 MW output power having a total electric efficiency of 46% for 230 s has been achieved in the development of the ITER gyrotron. High-power experiments were performed for TE<sub>19,7</sub> and TE<sub>25,9</sub> modes up to 2 s pulses. In the case of TE<sub>25,9</sub> mode, 1.0 MW output power was achieved at  $B_0 = 5.34$  T,  $V_{\text{beam}} = 76$  kV, and  $I_{\text{beam}} = 52$  A, and the output efficiency and total electric efficiency were  $\eta_{\text{out}} = 25.4\%$  and  $\eta_{\text{tot}} = 41.3\%$ , respectively. In the case of TE<sub>19,7</sub> mode, the output power reached 1.03 MW at  $B_0 = 4.04$  T,  $V_{\text{beam}} = 76$  kV, and  $I_{\text{beam}} = 53$  A, and the output efficiency and total electric efficiency were  $\eta_{\text{out}} = 25.5\%$  and  $\eta_{\text{tot}} = 40.0\%$ . Preliminary long-pulse experiments of TE<sub>37,13</sub> mode were also carried out using a small power supply system (up to 30 A beam current, 10 s duration). The achieved output power was still 0.42 MW for 5 s pulses at  $B_0 = 7.94$  T,  $V_{\text{beam}} = 72$  kV, and  $I_{\text{beam}} = 23.5$  A, and the output efficiency and total electric efficiency achieved were  $\eta_{\text{out}} = 25.1\%$  and  $\eta_{\text{tot}} = 38.5\%$ , respectively. High-power shots were also performed in the short-pulse operations (0.3 ms) and achieved a maximum power of 0.9 MW. There are also plans for long-pulse operations of 1 MW power at 203 GHz. As previously mentioned, the output efficiencies for sub-frequency are close to the efficiency of the main TE<sub>31,11</sub> mode under operation conditions. With four oscillation modes, stray power loss in the gyrotron was measured by the increase in temperature of the coolant. The stray power around the mode converter was mainly scattered toward the outside of gyrotron through a DC-break, acylinder made of silicon nitride. And, water flowing through a Teflon tube that is wound around the DC-break absorbs the stray power, while the stray power around the output window is absorbed by dummy loads that are connected to the main relief window and small viewing windows. The stray power ratio for the output power in each mode is listed in Table 4. The total stray power ratio was 9.4% for TE<sub>19,7</sub> mode, 6.0% for TE<sub>25,9</sub> mode, 3.4% for TE<sub>31,11</sub> mode, and 3.6% for TE<sub>37,13</sub> mode. The measured stray ratio for 137 and 104 GHz became 1.8 and 2.8 times that of 170 GHz, respectively. Since the curvature and

**Table 4** Measured stray power ratio at DC-break and relief windows for output power, and calculated transmission loss between internal mode converter and output window

TE <sub><i>m,n</i></sub> mode	19,7	25,9	31,11	37,13
Stray power at DC-break	5.9%	3.9%	2.4%	2.6%
Stray power at relief windows	3.5%	2.1%	1.0%	1.0%
Calculated transmission loss	4.5%	3.1%	1.5%	2.4%

size of the internal mirrors in the gyrotron are optimized for 170 GHz, the side lobe components of the larger beam generated by the increase in wavelength strayed from the surface area of internal mirrors and the aperture of the output window, which is consistent with the calculations. On the other hand, an increase of stray power loss in the 203 GHz oscillation was not observed and long-pulse operations comparable to that of 170 GHz oscillation can be expected. Ohmic loss ratio which was estimated by coolant temperature-rise in the mode converter and the internal mirrors were about 2% ~ 3% for each frequency and the values were not small. However, clear differences for each frequency were not obtained compared with measured stray RF power ratio. More detail measurements including ohmic losses at an inner wall in the gyrotron are needed.

## 4 Conclusion

Multi-frequency, MW power gyrotrons are essential devices in nuclear fusion science to control the electron temperature, plasma current, and stabilize plasma instabilities in various operating conditions. We have demonstrated a quad-frequency gyrotron of 104, 137, 170 and 203 GHz having a uniform directional beam by adopting the special mode group ( $TE_{19,7}$ - $TE_{25,9}$ - $TE_{31,11}$ - $TE_{37,13}$ ). The measured beam profiles were in agreement with the designed beam profile and the RF beams passed through the center of the output diamond window. High-power, long-pulse oscillations of 1.2 MW output power/27.5% output efficiency for 170 GHz, 1.0 MW output power/25.5% output efficiency for 104 and 137 GHz, and 0.4 MW output power/25% output efficiency for 203 GHz were achieved. In short pulses, a high-power shot of 0.9 MW at 203 GHz was reached. Moreover, 236 GHz oscillation by an upper oscillation mode ( $TE_{43,15}$  mode) in the same mode group may be also expected using a magnet having a higher magnetic field. This multi-frequency gyrotron offers 1 MW class operations over a broad frequency range for both large experimental devices of present (about 100 GHz) and future demo-class reactors (200 GHz range).

## References

1. M. Henderson, G. Saibene, C. Darbos, D. Farina, L. Figni, M. Gagliardi, F. Gandini, T. Gassmann, G. Hanson, A. Loarte, T. Omori, E. Poli, D. Purohit and K. Takahashi, *Phys Plasmas* 22, 021808 (2015).
2. K. Sakamoto, A. Kasugai, K. Takahashi, R. Minami, N. Kobayashi and K. Kajiwara, *Nature Phys.* 3 411 (2007).
3. A.G. Litvak, G.G. Denisov, V.E. Myasnikov, E.M. Tai, E.V. Sokolov and V.I. Ilin, *EPJ Web of Conferences*, 32, 04003 (2012).
4. I.Gr. Pagonakis, F. Albajar, S. Alberti, K. Avramidis, T. Bonicelli, F. Braunmueller, A. Bruschi, I. Chelis, F. Cismondi, G. Gantenbein, V. Hermann, K. Hesch, J.P. Hogge, J. Jelonnek, J. Jin, S. Illy, Z.C. Ioannidis, T. Kobarg, G.P. Latsas, F. Legrand, M. Lontano, B. Piosczyk, Y. Rozier, T. Rzesnicki, A. Samartsev, C. Schlatter, M. Thumm, I.G. Tigelis, M.Q. Tran, T.M. Tran, J. Weggen and J.L. Vomvoridis, *Eng. Des.* 96–97, 149 (2015).
5. K. Kajiwara, Y. Oda, A. Kasugai, K. Takahashi and K. Sakamoto, *Appl. Phys. Express* 4, 126001 (2011).
6. D. Wagner, G. Grünwald, F. Leuterer, A. Manini, F. Monaco, M. München, H. Schütz, J. Stober, H. Zohm, T. Franke, M. Thumm, G. Gantenbein, R. Heidinger, A. Meier, W. Kasperek, C. Lechte, A. Litvak, G.G. Denisov, A.V. Chirkov, E.M. Tai, L.G. Popov, V.O. Nichiporenko, V.E. Myasnikov, E.A. Solyanova, S.A. Malygin, F. Meo and P. Woskov, *Nucl. Fusion* 48, 054006 (2008).
7. T. Kobayashi, S. Moriyama K. Yokokura, M. Sawahata, M. Terakado, S. Hiranai, K. Wada, Y. Sato, J. Hinata, K. Hoshino, A. Isamaya, Y. Oda, R. Ikeda, K. Takahashi and K. Sakamoto, *Nucl. Fusion* 55 063008 (2015).

8. M. Thumm, A. Arnold, E. Borie, O. Braz, G. Dammertz, O. Dumbrajs, K. Koppenburg, M. Kuntze, G. Michel and B. Piosczyk, *Fusion Eng. Des.* 53, 407 (2001).
9. G. Gantenbein, A. Samartsev, G. Aiello, G. Dammertz, J. Jelonnek, M. Losert, A. Schlaich, T. Scherer, D. Strauss, M. Thumm and D. Wagner, *IEEE Trans. Electron Devices* 61, 1806 (2014).
10. K. Sakamoto, A. Kasugai, K. Takahashi, R. Minami, N. Kobayashi and K. Kajiwara, *Nat. Phys.* 3, 411 (2007).
11. M. V. Kartikeyan, E. Borie, and M. K. A. Thumm, *Gyrotrons*. Springer, New York, 2004.
12. R. Ikeda, K. Kajiwara, Y. Oda, K. Takahashi and K. Sakamoto, *Fusion Eng. Des.* 96–97, 482 (2015).